


 Cite this: *RSC Adv.*, 2023, **13**, 7731

## Controlling the crystal structure of succinic acid *via* microfluidic spray-drying†

 Aysu Ceren Okur,<sup>a</sup> Philipp Erni,<sup>b</sup> Lahoussine Ouali,<sup>b</sup> Daniel Benczedi<sup>b</sup> and Esther Amstad<sup>a</sup> 

Many properties of materials, including their dissolution kinetics, hardness, and optical appearance, depend on their structure. Unfortunately, it is often difficult to control the structure of low molecular weight organic compounds that have a high propensity to crystallize if they are formulated from solutions wherein they have a high mobility. This limitation can be overcome by formulating these compounds within small airborne drops that rapidly dry, thereby limiting the time molecules have to arrange into the thermodynamically most stable phase. Such drops can be formed with a surface acoustic wave (SAW)-based spray-drier. In this paper, we demonstrate that the structure of a model low molecular weight compound relevant to applications in pharmacology and food, succinic acid, can be readily controlled with the supersaturation rate. Succinic acid particles preserve the metastable structure over at least 3 months if the initial succinic acid concentration is below 2% of its saturation concentration such that the supersaturation rate is high. We demonstrate that also the stability of the metastable phases against their transformation into the most stable phase increases with decreasing initial solute concentration and hence with increasing supersaturation rate of the spray-dried solution. These insights open up new opportunities to control the crystal structure and therefore properties of low molecular weight compounds that have a high propensity to crystallize.

 Received 10th October 2022  
 Accepted 1st March 2023

DOI: 10.1039/d2ra06380h

[rsc.li/rsc-advances](http://rsc.li/rsc-advances)

## Introduction

Many physicochemical properties of materials that determine their appearance and performance, such as their color,<sup>1–3</sup> conductivity,<sup>4</sup> density<sup>5</sup> and solubility<sup>6,7</sup> depend on their structure. For example, the dissolution kinetics and hence bioavailability of many poorly soluble drugs increases if formulated as a metastable phase.<sup>6,8</sup> The structure of low molecular weight organic materials is often controlled with additives. However, these additives typically increase product cost and reduce the efficiency of active ingredients because they dilute them. To mitigate these shortcomings, the structure of materials can be controlled through their processing. For example, active pharmaceutical ingredients (APIs) have been processed into amorphous particles through ball milling<sup>9–11</sup> or freeze drying.<sup>12</sup> However, ball milling risks to introduce impurities and freeze drying is costly. A cheap, high throughput method that offers some control over the structure of the resulting particles is bulk recrystallization. This technique was used, for example, to formulate carbamazepine (CBZ) as a metastable phase.<sup>13</sup> Yet,

even if formulated as a metastable phase, its dissolution kinetics is slow such that its bioavailability is compromised. This shortcoming can be addressed by co-crystallizing the active ingredient with more soluble low molecular weight excipients such as succinic acid. Unfortunately, the high propensity of low molecular weight excipients to crystallize risks phase separations and ultimately disproportionation which makes bulk processing time consuming. Moreover, uncontrolled phase separations render the control over the structure of the forming materials challenging. A means to overcome this limitation is spray drying.<sup>14,15</sup> The crystal structure of these compounds can be tuned with the processing temperature, initial solute concentration, solvent evaporation rate, and solvent quality.<sup>16–18</sup> To increase the bioavailability of many of these actives, they are often co-spray dried with low molecular weight additives such as succinic acid<sup>19</sup> Indeed, many active ingredients including carbamazepine,<sup>19,20</sup> nicotinamide<sup>20,21</sup> and salbutamol sulfate<sup>22,23</sup> are co-spray dried with some excipients such as lactose<sup>22,24</sup> and mannitol.<sup>25–28</sup> Unfortunately, it becomes much more difficult to control the crystal structure and hence properties of active ingredients if they are co-spray-dried with excipients. To enable a more reliable formulation of low molecular weight organic active ingredients as metastable phases, systematic studies on the influence of the spray drying conditions on the structure of these materials and their storage stability are warranted. These studies are strongly facilitated if spray-drying can be performed

<sup>a</sup>Soft Materials Laboratory, Institute of Materials, École Polytechnique Fédérale de Lausanne (EPFL), Lausanne 1015, Switzerland. E-mail: esther.amstad@epfl.ch

<sup>b</sup>Firmenich SA, Corporate R&D Division, PO Box 239, CH-1211 Geneva 8, Switzerland

† Electronic supplementary information (ESI) available. See DOI: <https://doi.org/10.1039/d2ra06380h>



on a small scale where the processing conditions can be more closely controlled.

In this paper, we employ a microfluidic surface acoustic wave (SAW)-based spray-dryer to investigate the influence of the spray-drying conditions on the structure of a model low molecular weight matrix material, as schematically shown in Fig. 1. The SAW-based spray drier forms small drops with diameters between 10 and 100  $\mu\text{m}$ .<sup>29,30</sup> The evaporation rate scales with the surface to volume ratio of the drop. Due to the very small size of these drops, they dry within a few hundred milliseconds,<sup>31</sup> thereby giving access to length and time scales for materials synthesis and formulations that cannot be reached using traditional macroscopic spray-drying processes. We demonstrate that the structure of succinic acid, a model low molecular weight matrix material, and its stability against crystallization during storage under ambient conditions can readily be controlled with the time it has to solidify and hence, the supersaturation rate. Moreover, we find that the initial solute concentration strongly influences the stability of metastable spray-dried particles against the transformation into a more stable polymorph. This finding might open up new avenues for the formulation of carrier particles that efficiently retain low molecular weight substances, including volatiles, without the need for costly additives or time-consuming processes.

## Results and discussion

### Spray drying of succinic acid nanoparticles

To control the formation time of particles, they are generated with a SAW-based spray-drier we previously introduced.<sup>30</sup> The SAW device produces airborne drops with diameters between 1 and 10  $\mu\text{m}$  that dry within a few hundred ms,<sup>32</sup> if operated at a frequency of 64.5 MHz.<sup>30</sup> These drops are guided into a drying unit within which room temperature air co-flows with the drops before the dry particles are collected on a silicon wafer that is placed close to the top end of the drying tube within few seconds, as schematically shown in Fig. 2.<sup>30</sup>

The time needed for low molecular weight solutes to diffuse the length of the initial radius of the drop is similar to the time needed to dry it. Hence, we approximate the solute



Fig. 1 Schematic illustration of the microfluidic spray dryer. Liquid is controllably delivered onto the chip through a PDMS-based channel before it is atomized. The resulting drops enter the drying tube.<sup>30</sup>

concentration within the drop to be constant such that we expect to obtain solid spray-dried particles. Under these conditions, solutes start to solidify when their overall concentration exceeds their saturation concentration and their formation is arrested when the drop is dried.<sup>33</sup> The time when the saturation concentration is reached within the drying drop depends on the solubility of the solute and its initial concentration.

We employ succinic acid as a model matrix material because it is a well-suited matrix material for the encapsulation of volatile compounds, and co-crystallization of pharmaceuticals.<sup>34,35</sup> Succinic acid is a dicarboxylic acid that has three polymorphs, the metastable  $\alpha$  and  $\gamma$  and the stable  $\beta$  polymorph.<sup>36,37</sup> We dissolve succinic acid in ethanol and vary its initial concentration from 10 mM to 100 mM, corresponding to 2–20% of its saturation concentration. This solution is injected into a poly(dimethyl siloxane) (PDMS)-based channel that guides it onto a SAW-based spray-drier at a rate of 1.5 ml  $\text{h}^{-1}$ . The SAW device breaks the solution into airborne drops that dry within a few hundred ms.<sup>29,30</sup> The resulting spray dried particles are spherical, independent of the initial solute concentration, as shown in the scanning electron microscopy (SEM) images in Fig. 3A and B, and well in agreement with what we previously reported.<sup>29</sup> Because each drop forms exactly one particle,<sup>30,38</sup> the size of these particles scales with the initial solute concentration: particles produced from solutions containing 10 mM succinic acid have an average diameter of 150 nm whereas those produced from solutions containing 100 mM succinic acid have an average diameter of 250 nm,<sup>29</sup> as exemplified in Fig. 3. The good correlation between the initial solute concentration and the size of spray-dried particles confirms that each drop forms exactly one particle and that these particles do not have a core-shell structure.

To test the influence of the initial solute concentration on the structure of the resulting particles, we perform X-ray diffraction (XRD) analysis. Particles produced from 10 mM succinic acid containing solutions predominantly display the metastable  $\alpha$  phase, as demonstrated by the diffraction peak at  $2\theta = 22^\circ$ . By contrast, particles formulated from 100 mM succinic acid containing solutions display predominantly the stable  $\beta$  phase, as shown by the diffraction peak at  $2\theta = 20^\circ$  in Fig. 3C.<sup>37</sup> These results indicate that the structure of spray-dried succinic acid particles depends on their formation time and hence the supersaturation rate which can be tuned with the initial solute concentration.

Our results suggest that the structure of succinic acid particles formulated with the SAW-based spray-drier can be controlled *via* the supersaturation rate. This rate is closely related to the drying time of the drops and hence the vapor pressure of their constituent solvent. To elucidate how the drying time of the drops influences the structure of spray-dried succinic acid particles, we form drops from solvents that have different vapor pressures, namely deionized water, ethanol and acetone. All spray-dried particles are spherical, as shown in Fig. 4A–F. Particles produced from solutions initially containing 10 mM succinic acid are predominantly metastable, independent of the solvent used, as shown in Fig. 4G. If formulated from



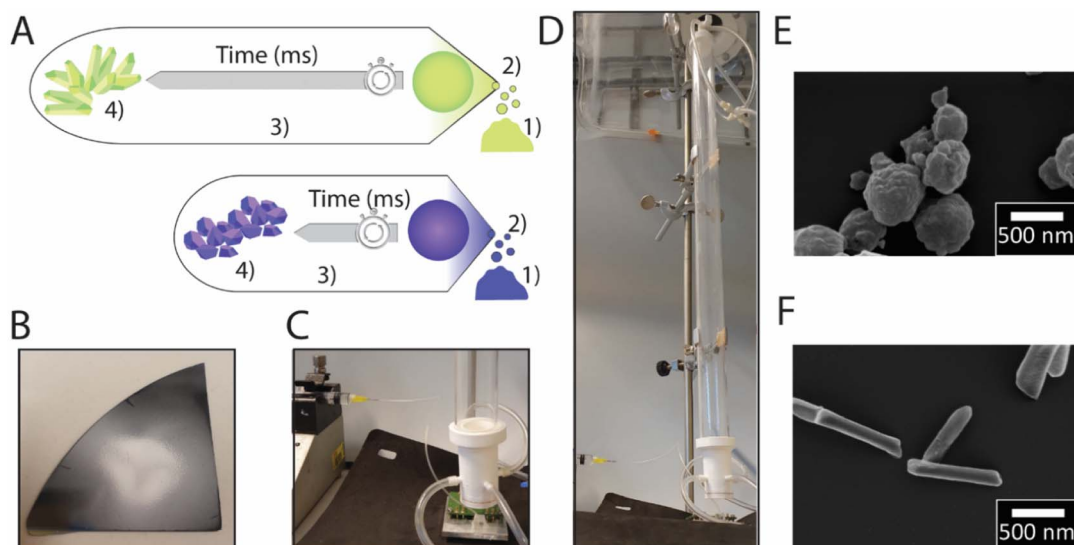


**Fig. 2** (A) Schematic illustration of succinic acid particles spray-dried from solvents with different vapor pressures that result in particles displaying different crystal structures. The solute-containing solvent is delivered onto the SAW device where it is broken into (1) airborne drops (2) that are guided into the drying unit (3) where solutes start to solidify. By adjusting the drying tube length, we ensure that all the solvent is evaporated before the dried particles are deposited onto a substrate (4). (B) Silicon wafer substrate containing collected nanoparticles. The SAW-based setup consists of (C) a microfluidic PDMS channel into which liquid is fed using a syringe pump and (D) a drying glass tube within which drops dry while travelling to the collection substrate. (E and F) SEM micrographs of succinic acid particles produced from ethanol-based solutions initially containing 100 mM succinic acid when dried from small aerosol drops (E) within the drying unit (F) at room temperature.

such diluted solutions where the initial succinic acid concentration is between 1.5 and 4% of its saturation concentration, the supersaturation rate is very high such that the formation of the stable  $\beta$  phase is kinetically prevented even if solvents with high vapor pressures are used. If we increase the initial solute concentration to 100 mM, particles are still predominantly metastable if formulated from ethanol-based solutions, where the initial succinic acid concentration is as low as 20% of its saturation concentration such that the supersaturation rate is still high. By contrast, if formulated from acetone-based solutions, where the initial succinic acid concentration corresponds to 40% of its saturation concentration and hence, the supersaturation rate is lower, a significant fraction of the particles displays the stable  $\beta$  phase. The fraction of stable particles is

even higher if formulated from aqueous solutions, where the initial concentration corresponds to 15% of its saturation concentration, as shown in Fig. 4H. We assign this difference in structure to the different drying rates of the solvents: water has a lower vapor pressure of 3.16 kPa at room temperature,<sup>39</sup> compared to ethanol, whose vapor pressure is 7.87 kPa,<sup>40</sup> such that aqueous drops dry much more slowly. The slower drop drying results in lower supersaturation rates such that succinic acid molecules have more time to arrange into the stable phase. Hence, the fraction of stable particles is much larger than if formulated from ethanol-based solutions where the supersaturation rate is much higher even if particles start precipitating later during the drop drying process.

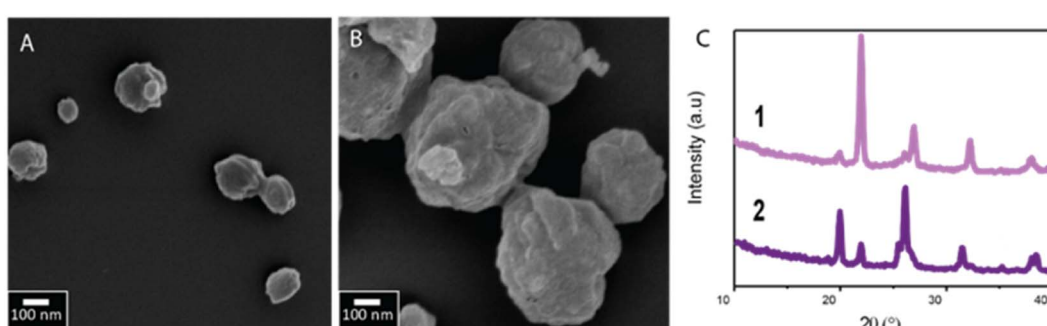


**Fig. 3** Structure and morphology of succinic acid particles. SEM image of succinic acid particles produced from ethanol-based solutions initially containing (A) 10 mM and (B) 100 mM succinic acid, corresponding to (A) 2 and (B) 20% of its supersaturation concentration. (C) Crystal structure of spray-dried particles produced from solutions initially containing (1) 10 mM and (2) 100 mM succinic acid. The diffractogram suggests that the spray-dried particles are in the metastable  $\alpha$  phase, as demonstrated by the diffraction peak at  $2\theta = 22^\circ$  and the stable  $\beta$  phase, as shown by the diffraction peak at  $2\theta = 20^\circ$ .



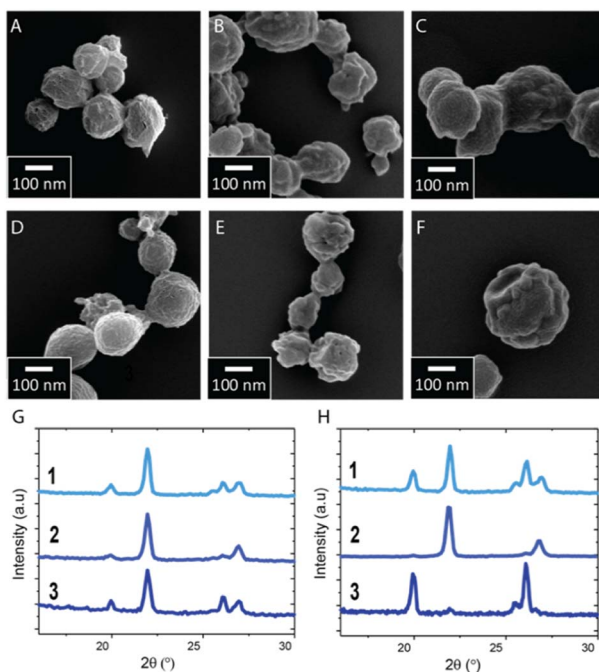


Fig. 4 (A–F) Morphology and (G and H) crystal structures of spray-dried succinic acid particles produced from (A and D) DI water, (B and E) ethanol, and (C and F) acetone containing (A–C) 10 mM and (E–G) 100 mM succinic acid. XRD traces of succinic acid particles spray-dried from (1) acetone, (2) ethanol and (3) DI water initially containing (G) 10 mM and (H) 100 mM succinic acid.

### Stability of crystal structure during storage

Metastable structures typically tend to transform into the stable phase over time. The rate at which this phase transformation occurs depends on the mobility of the molecules within the metastable phase. In addition, it depends on the density and size of nuclei possessing the stable phase that might be present within the metastable matrix but are invisible with XRD because

their size or density is below its detection limit. We expect the density of stable nuclei to increase with decreasing supersaturation rate and hence initial solute concentration. To test this expectation, we compare the stability of succinic acid particles spray-dried from ethanol-based solutions initially containing 10 and 100 mM succinic acid. Indeed, particles produced from solutions initially containing 10 mM succinic acid, that have been processed at a high supersaturation rate, preserve their metastable structure for more than three months if stored at 25 °C and 40% relative humidity. By contrast, if sprayed from solutions initially containing 100 mM succinic acid, where the supersaturation rate was slow, the majority of particles transforms from the metastable to the stable phase within 20 h if stored under identical conditions, as shown in Fig. 5B. These results indicate that metastable particles that have been processed at low supersaturation rates encompass stable nuclei. Yet, these nuclei are not detectable with XRD if analyzed within a few hours after production.

To quantify the influence of the initial solute concentration on the structural stability, we monitor the ratio of the intensities of the diffraction peaks at  $2\theta = 20^\circ$ :  $2\theta = 22^\circ$ , corresponding to the rate of the phase transformation from the metastable into the stable phase. Indeed, the rate of phase transformation increases with increasing initial solute concentration and hence decreasing supersaturation rate, as shown in Fig. 5C. These results suggest that with decreasing supersaturation rate, the density of nuclei possessing the stable  $\beta$  phase, increases. These nuclei grow over time at the expense of the metastable phase, until the vast majority of the particles possesses the stable  $\beta$  phase.

### Influence of additives on crystal structure of succinic acid

A key advantage of the spray-drying process is the ability to load matrix materials with well-defined amounts of active ingredients because each drop forms exactly one particle such that the particle composition corresponds to that of the solute

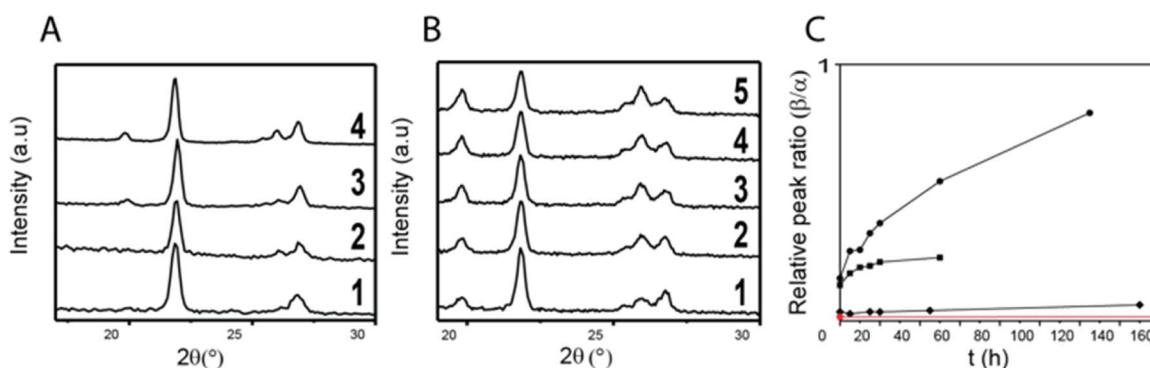


Fig. 5 Influence of the initial solute concentration on the structural stability of spray-dried particles. XRD traces of particles spray-dried from solutions initially containing (A) 10 mM and (B) 100 mM succinic acid. Particles produced from 10 mM succinic acid containing solutions have been characterized at (1)  $t = 0$  h (2)  $t = 2$  weeks (3)  $t = 1$  month (4)  $t = 3$  months. Those produced from solutions initially containing 100 mM succinic acid have been characterized after (1)  $t = 0$  h, (2)  $t = 5$  h, (3)  $t = 10$  h, (4)  $t = 15$  h and (5)  $t = 20$  h. (C) Overview of the evolution of the structure of particles produced from ethanol-based solutions initially containing (●) = 100 mM, (■) = 75 mM, (◆) = 50 mM and (●') = 10 mM succinic acid if stored at ambient conditions. Relative peak ratio indicates the transformation rate of succinic acid from the metastable  $\alpha$  phase to the stable  $\beta$  phase.



concentration.<sup>30,32,41</sup> The structure of spray-dried particles often depends on additives present during their formulation.<sup>42</sup> To check if active ingredients also influence the structure of spray-dried succinic acid, we employ vanillin, a volatile low molecular weight compound, as a model additive. Upon spray-drying of an ethanol-based solution containing 60 mM vanillin and 100 mM succinic acid, we obtain highly irregular particles. Particles made from ethanol-based solutions initially containing 100 mM succinic acid display needle-like structures if stored under ambient conditions for 24 hours, as shown in Fig. 6A. Particles encompassing vanillin have a higher density of needles than those without vanillin, as shown in Fig. 6B. These results suggest that the needle-like structures are based on succinic acid. Indeed, if succinic acid is slowly dried at room temperature, we obtain the  $\beta$  phase that exhibits needle-like structures, as shown in Fig. 2F.<sup>43</sup> These results suggest that vanillin acts as heterogeneous nucleation sites for succinic acid crystals. By contrast, spray-dried pure vanillin particles are spherical, as shown in Figure S1.<sup>†</sup> These results indicate that by controlling the supersaturation rate of succinic acid, for example by tuning the spray-drying conditions, we can control the crystal structure and particle morphology.

The heterogeneous morphology of succinic acid-based particles that have been co-spray dried with vanillin suggests that these two compounds phase separate while the drops dry. We expect this phase separation to only occur if the vanillin to succinic acid concentration ratio exceeds a threshold value. To test this expectation, we vary the initial vanillin concentration from 10 mM to 60 mM, corresponding to a saturation concentration of 3 to 20% while keeping the initial succinic acid concentration constant at 100 mM, corresponding to a supersaturation concentration of 20%. To monitor the phase

separation, we perform XRD analysis on the spray-dried samples. We observe a diffraction peak at  $2\theta = 13^\circ$ , characteristic for vanillin, if the initial vanillin concentration exceeds 15 mM, as shown in Fig. 6D, suggesting that macroscopic phase separations start to occur at this concentration. Note that the rate of phase transformation of the metastable  $\alpha$  into the stable  $\beta$  phase increases with increasing amount of vanillin present in these particles, as shown in Fig. 6E. These results confirm that vanillin acts as heterogeneous nucleation sites, thereby promoting the formation of succinic acid nuclei possessing the stable phase.

Phase separations are typically specific to a given combination of solutes and solvents such that they must be assessed case-by-case. To demonstrate that SAW-based spray-drying is a suitable technique to formulate different types of volatile-loaded succinic acid particles, we co-spray dry succinic acid with another volatile, maltol. Remarkably, by contrast to vanillin, maltol increases the stability of the metastable  $\alpha$  phase of succinic acid such that it remains in this form for at least one week if produced from ethanol-based solutions initially containing 60 mM maltol and 100 mM succinic acid, as shown in Fig. 5E. These results indicate that SAW-based spray-drying enables the formulation of succinic acid-based particles that can efficiently be controlled with different types of volatile additives.

## Experimental section

### Solution preparation

Vanillin, maltol, acetone (technical grade), and ethanol (absolute grade) are purchased from Sigma Aldrich, succinic acid from Merck. We employ deionized water from Direct-Q Merck Millipore 25 °C, 0.05  $\mu$ S cm<sup>-1</sup>. All reagents are used as received.

Succinic acid-based particles are formulated from acetone, ethanol or deionized water (DI)-based solutions containing 10–100 mM succinic acid. To test the influence of active ingredients on the morphology of succinic acid particles, an ethanol-based solution containing various amounts of vanillin and maltol and 100 mM of succinic acid is spray dried. To test the influence of active ingredients on the structural stability, ethanol-based solutions containing 100 mM succinic acid and either 20–60 mM vanillin or 60 mM maltol are spray dried.

### Spray-drying operation

Particles are produced using a surface acoustic wave (SAW)-based spray-drying method. The device is composed of a LiNbO<sub>3</sub> wafer with a size of 2 × 3 cm<sup>2</sup> onto which an Inter-digital transducer (IDT) finger cross pattern is sputtered as described previously.<sup>30</sup> The wafer is connected to a PowerSAW Generator (Bekeltronig GmbH) via a Printed Circuit Board (PCB). The solution is delivered onto the chip through a poly(dimethylsiloxane) (PDMS) (Sylgard 184, Dow Corning) based microfluidic channel that is bound to the piezoelectric wafer using oxygen plasma. The solution is injected into the PDMS-based channel with a width and height of 100  $\mu$ m using a volume-controlled syringe pump (Cronus Sigma 1000, Labhut)

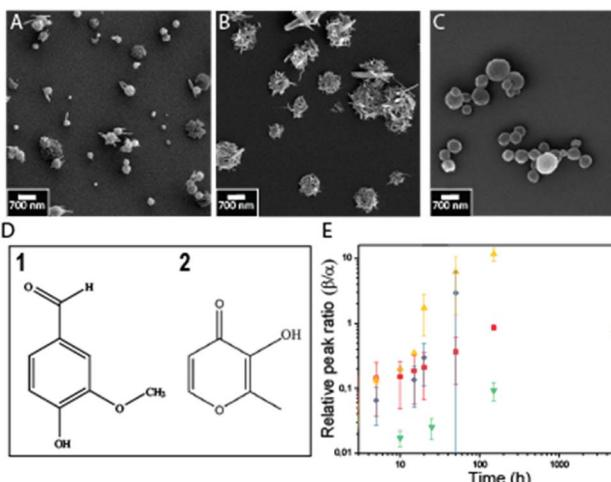


Fig. 6 SEM image of succinic acid particles spray dried (A) in the absence of vanillin, with 60 mM (B) vanillin and (C) maltol. (D) Molecular structures of (1) vanillin and (2) maltol. (E) Evolution of the crystal structure of vanillin loaded succinic acid particles initially containing 100 mM succinic acid and (▲) 60 mM, (●) 20 mM, (■) 0 mM of vanillin and (▼) 60 mM of maltol. Relative peak ratio represents the ratio of the intensities of the diffraction peaks at  $2\theta = 20^\circ$ :  $2\theta = 22^\circ$ , where 20° represents stable, 22° represents metastable phase.



at a flow rate of 1.5 ml h<sup>-1</sup>. The powerSAW Generator is operated at 3.3 W. The dried particles are collected on one side polished silicon wafers for further characterization.

## Characterization

**Scanning electron microscopy (SEM).** Samples are imaged with a scanning electron microscope (Zeiss Merlin field emission SEM) operated at an acceleration voltage of 2 kV and 100 pA using an in-lens detector. To avoid charging effects, the samples are coated with a 4 nm thick iridium film (Quorum Q 150).

**X-ray diffraction (XRD).** The structural stability of spray dried particles is characterized as a function of time using powder X-ray diffraction (pXRD). Particles are collected on a one-side polished single crystal silicon wafer that does not yield any 2 $\theta$  peak in the region of interest (10–30°) and stored under ambient conditions. They are characterized with an Empyrean X-ray diffractometer (PANalytical) with PIXcel-1D detector using a Cu K $\alpha$  source with a wavelength of 1.5405 Å.

## Conclusions

We demonstrate that the structure and the structural stability during storage of a model low molecular weight organic matrix material, succinic acid, strongly depend on its processing conditions. SAW-based microfluidic spray-drying enables the formulation of succinic acid into the metastable  $\alpha$  phase without the need for any crystallization inhibiting additives. Importantly, if formulated within micrometer-sized drops that rapidly dry such that the supersaturation rate is high, the metastable phase is much more stable against crystallization during storage at room temperature than if formulated at low supersaturation rates, for example in larger drops or drops that dry more slowly. These findings open up new possibilities to tune the dissolution kinetics of matrix materials composed of low molecular weight organic compounds that efficiently retain volatile substances and thereby their release kinetics by adjusting spray-drying conditions.

## Conflicts of interest

There are no conflicts to declare.

## Acknowledgements

This research is funded by Firmenich SA.

## References

- 1 B. A. Nogueira, C. Castiglioni and R. Fausto, *Commun. Chem.*, 2020, **3**, 34.
- 2 X. Li, X. Ou, B. Wang, H. Rong, B. Wang, C. Chang, B. Shi, L. Yu and M. Lu, *Commun. Chem.*, 2020, **3**, 152.
- 3 M. Cavallini, A. Calò, P. Stoliar, J. C. Kengne, S. Martins, F. C. Matacotta, F. Quist, G. Gbabode, N. Dumont, Y. H. Geerts and F. Biscarini, *Adv. Mater.*, 2009, **21**, 4688–4691.
- 4 L. Hildebrandt, R. Dinnebier and M. Jansen, *Inorg. Chem.*, 2006, **45**, 3217–3223.
- 5 S. Sobczak, P. Ratajczyk and A. Katrusiak, *Chem.-Eur. J.*, 2021, **27**, 7069–7073.
- 6 R. Censi and P. Di Martino, *Molecules*, 2015, **20**, 18759–18776.
- 7 M. Pudipeddi and A. T. M. Serajuddin, *J. Pharm. Sci.*, 2005, **94**, 929–939.
- 8 G. Van den Mooter, *Drug Discovery Today: Technol.*, 2012, **9**, e79–e85.
- 9 K. Löbmann, H. Grohganz, R. Laitinen, C. Strachan and T. Rades, *Eur. J. Pharm. Biopharm.*, 2013, **85**, 873–881.
- 10 K. T. Jensen, K. Löbmann, T. Rades and H. Grohganz, *Pharmaceutics*, 2014, **6**, 416–435.
- 11 D. Modhave, I. Saraf, A. Karn and A. Paudel, *AAPS PharmSciTech*, 2020, **21**, 152.
- 12 M. Wostry, H. Plappert and H. Grohganz, *Pharmaceutics*, 2020, **12**, 941.
- 13 F. Flicker, V. A. Eberle and G. Betz, *Pharmaceutics*, 2012, **4**, 58–70.
- 14 R. A. Halliwell, R. M. Bhardwaj, C. J. Brown, N. E. B. Briggs, J. Dunn, J. Robertson, A. Nordon and A. J. Florence, *J. Pharm. Sci.*, 2017, **106**, 1874–1880.
- 15 B. Long, G. M. Walker, K. M. Ryan and L. Padrela, *Cryst. Growth Des.*, 2019, **19**, 3755–3767.
- 16 S. Dohrn, P. Rawal, C. Luebbert, K. Lehmkemper, S. O. Kyeremateng, M. Degenhardt and G. Sadowski, *Int. J. Pharm.: X*, 2021, **3**, 100072.
- 17 N. Li, J. L. Cape, B. R. Mankani, D. Y. Zemlyanov, K. B. Shepard, M. M. Morgen and L. S. Taylor, *Mol. Pharm.*, 2020, **17**, 4004–4017.
- 18 T. Huppertz and I. Gazi, *J. Dairy Sci.*, 2016, **99**, 6842–6851.
- 19 M. Ullah, H. Ullah, G. Murtaza, Q. Mahmood and I. Hussain, *BioMed Res. Int.*, 2015, **2015**, 870656.
- 20 S. P. Patil, S. R. Modi and A. K. Bansal, *Eur. J. Pharm. Sci.*, 2014, **62**, 251–257.
- 21 H. M. Tawfeek, T. Chavan and N. K. Kunda, *AAPS PharmSciTech*, 2020, **21**, 181.
- 22 M. S. Ferdynand and A. Nokhodchi, *Drug Delivery Transl. Res.*, 2020, **10**, 1418–1427.
- 23 D. O. Corrigan, O. I. Corrigan and A. M. Healy, *Int. J. Pharm.*, 2004, **273**, 171–182.
- 24 L. Wu, X. Miao, Z. Shan, Y. Huang, L. Li, X. Pan, Q. Yao, G. Li and C. Wu, *Asian J. Pharm. Sci.*, 2014, **9**, 336–341.
- 25 A. Buanz, M. Gurung and S. Gaisford, *CrystEngComm*, 2019, **21**, 2212–2219.
- 26 T. F. Guimarães, A. D. Lanchote, J. S. da Costa, A. L. Viçosa and L. A. P. de Freitas, *Adv. Powder Technol.*, 2015, **26**, 1094–1101.
- 27 W. L. Hulse, R. T. Forbes, M. C. Bonner and M. Getrost, *Int. J. Pharm.*, 2009, **382**(1–2), 67–72.
- 28 E. M. Littringer, A. Mescher, S. Eckhard, H. Schröttner, C. Langes, M. Fries, U. Griesser, P. Walzel and N. A. Urbanetz, *Drying Technol.*, 2012, **30**, 114–124.
- 29 A. C. Okur, P. Erni, L. Ouali, D. Benczedi and E. Amstad, *ACS Sustainable Chem. Eng.*, 2022, **10**, 2914–2920.



30 M. Steinacher, H. Du, D. Gilbert and E. Amstad, *Adv. Mater. Technol.*, 2019, **4**, 1800665.

31 J. Wei and Y. Li, *Build. Environ.*, 2015, **93**, 86–96.

32 H. Du, M. Steinacher, C. Borca, T. Huthwelker, A. Murello, F. Stellacci and E. Amstad, *J. Am. Chem. Soc.*, 2018, **140**, 14289–14299.

33 J. McGinty, N. Yazdanpanah, C. Price, J. H. ter Horst and J. Sefcik, in *The Handbook of Continuous Crystallization*, The Royal Society of Chemistry, 2020, pp. 1–50.

34 M. Ullah, I. Hussain and C. C. Sun, *Drug Dev. Ind. Pharm.*, 2016, **42**(6), 969–976.

35 Y. Tang, H. B. Scher and T. Jeoh, *ACS Food Sci. Technol.*, 2021, **1**, 2086–2095.

36 P. Lucioli, E. Nauha, I. Gimondi, L. S. Price, R. Guo, L. Iuzzolino, I. Singh, M. Salvalaglio, S. L. Price and N. Blagden, *CrystEngComm*, 2018, **20**, 3971–3977.

37 Q. Yu, L. Dang, S. Black and H. Wei, *J. Cryst. Growth*, 2012, **340**, 209–215.

38 E. Amstad, M. Gopinadhan, C. Holtze, C. O. Osuji, M. P. Brenner, F. Spaepen and D. A. Weitz, *Science*, 2015, **349**, 956–960.

39 A. Wexler, *J. Res. Natl. Bur. Stand. A Phys. Chem.*, 1976, **80A**, 775–785.

40 C. B. Kretschmer and R. Wiebe, *J. Am. Chem. Soc.*, 1949, **71**, 1793–1797.

41 E. Amstad, M. Gopinadhan, C. Holtze, C. O. Osuji, M. P. Brenner, F. Spaepen and D. A. Weitz, *Science*, 2015, **349**, 956–960.

42 M. Dixit, P. Kulkarni, A. Kini and H. Shivakumar, *Int. J. Drug Formul. Res.*, 2010, **1**, 1–29.

43 D. Setyawan, A. Paramanandana, V. Erfadrian, R. Sari and D. Paramita, *J. Res. Pharm.*, 2020, **24**(3), 410–415.

